Design of a MEMS sensor array for dam subsidence monitoring based on dual-sensor cooperative measurements

Tao Tao[1], Jianfeng Yang[1], Wei Wei[2*], Marcin Woźniak[3], Rafał Scherer[4], and Robertas Damaševičius[5]

[1]School of Electronic Information, Wuhan University
Wuhan, Hubei, 430060, China
[e-mail: taotao1295@163.com]
[2] School of Computer Science and Engineering, Xi'an University of Technology
Xi'an, Shaanxi, 710048, China
[e-mail: weiwei@xaut.edu.cn]
[3]FACULTY OF APPLIED MATHEATICS s, Silesian University of Technology,
Kaszubska 23, Gliwice, 44-100, Poland.
[e-mail: marcin.wozniak@polsl.pl]
[4]Czestochowa University of Technology Al.
Armii Krajowej 36, Czestochowa, 42-200, Poland
[e-mail:rafal.schererg@pcz.pl]
[5]Faculty of Informatics, Multimedia Engineering Department, Kaunas University of Technology,
Kaunas, LT-04340, Lithuania
[e-mail: robertas.damasevicius@ktu.lt]
*Corresponding author: Wei Wei

Received November 6, 2020; revised January 6, 2021; revised February 16, 2021; revised March 30, 2021; accepted August 2, 2021; published October 31, 2021

Abstract

With the rapid development of the Chinese water project, the safety monitoring of dams is urgently needed. Many drawbacks exist in dams, such as high monitoring costs, a limited equipment service life, long-term monitoring difficulties. MEMS sensors have the advantages of low cost, high precision, easy installation, and simplicity, so they have broad application prospects in engineering measurements. This paper designs intelligent monitoring based on the collaborative measurement of dual MEMS sensors. The system first determines the endpoint coordinates of the sensor array by the coordinate transformation relationship in the monitoring system and then obtains the dam settlement according to the endpoint coordinates. Next, this paper proposes a dual-MEMS sensor collaborative measurement algorithm that builds a mathematical model of the dual-sensor measurement. The monitoring system realizes mutual compensation between sensor measurement data by calculating the motion constraint matrix between the two sensors. Compared with the single-sensor measurement, the dual-sensor measurement algorithm is more accurate and can improve the reliability of long-term monitoring data. Finally, the experimental results show that the dam subsidence monitoring system proposed in this paper fully meets the engineering monitoring accuracy needs, and the dual-sensor collaborative measurement system is more stable than the single-sensor monitoring system.

http://doi.org/10.3837/tiis.2021.10.005 **ISSN : 1976-7277**

Keywords: Dam monitoring system, MEMS sensor arrays, Cooperative measurement with dual-sensors, Subsidence monitoring, Platform to realize

1. Introduction

China is the world's leading country in dam engineering technology. At present, China has built nearly 100, 000 reservoir dams. On the one hand, constructing dams can bring huge economic benefits but, on the other hand, will bring serious outcomes to mankind if the dam fails [1]. In August 2012, a 180, 000 m3 containment reservoir experienced dam failure in Zhoushan City, Zhejiang Province. The dam failure accident occurred suddenly, and water and sediment mixed with mud fell down, causing many downstream houses to be washed away. Several people were buried, 11 people were killed and 27 were injured [2].

Dam safety monitoring refers to obtaining relevant data of the dam by professional equipment and manual inspections to ensure that the dam can achieve its maximum benefit under safe conditions [3-4]. Dam safety monitoring can be traced back to the end of the 19th century, when German engineers observed the horizontal displacement of the Eschbach gravity dam in 1891. As researchers from various countries have subsequently researched dam safety monitoring, dam safety monitoring systems have gradually improved. The initial dam safety monitoring methods included appearance inspection, single-point monitoring, and qualitative analysis, while we currently obtain data and quantitatively analyses the safety of dams using high-precision instruments. The conventional monitoring methods are lead-type horizontal displacement meters, pipe-type sedimentation meters and fixed inclinometers used for measurements. The conventional methods are cumbersome, time-consuming and labor-intensive and have a low degree of automation, serious interference from human causes, and difficult data processing, so they do not meet the requirements of the fast, real-time and dynamic monitoring of dam deformation [5-6].

With the development of microelectromechanical systems (MEMS), MEMS sensors have been widely used in civil engineering. MEMS sensors originated in the 1950s. Discovering the piezoresistive effect of Si semiconductors, researchers began their research on Si sensors. Based on the development of MEMS, the piezoresistive effect of Si semiconductors is used to convert the changes of features such as pressure, displacement, acceleration and angle into the changes of voltage in the circuit so that it is convenient to calculate the displacement and angle of the monitoring point. In 1962, the coming of the first miniature silicon pressure sensor created a precedent for MEMS technology. The continuous development of MEMS technology has also promoted improvements in sensor performance [7-9].

Professor CEYLAN from Iowa State University proposed the idea of a "smart road". During road paving, wireless MEMS sensors are embedded in the concrete to realize the real-time monitoring of road temperature, humidity and other criteria [10]. C Li carried out research on ground subsidence monitoring technology based on MEMS sensor data fusion for the

tunnel during the shield construction period. Based on this method, by arranging the sensor node monitoring network, the absolute surface settlement caused by tunnel construction can be estimated. [11]. Taiwan's National Earthquake Engineering Research Center LIN and others have developed a local bridge scour safety system that is based on ZigBee network technology and MEMS sensor technology and that integrates MEMS acceleration sensors and MEMS pressure sensors for bridge health monitoring [12]. Zhu HC proposed a set of in situ and long-term submarine terrain deformation monitoring systems. The scheme of using a MEMS attitude sensor to form arrays for in situ and long-term monitoring was determined. The selection of key parts was described in detail, and the related hardware and system structure were designed. This system realized the rapid collection of multimode and long-distance data [13]. Liu FC designed array displacement meter-based slope deformation monitoring for pumped energy storage power stations, whose main monitoring unit is a shape array accelerometer produced in Canada. The Shape Accel Array (SAA) converts the acceleration change monitored by the accelerometer into displacement through a quadratic integral [14]. To address the lack of conventional monitoring instruments, Liao C proposed an FOG strap down inertial navigation system combining an FOG and accelerometer to monitor dam body deformation and measure the tilt value of an object according to varying angles. However, this system is not suitable for long-term real-time monitoring [15].

MEMS sensors can achieve long-term real-time monitoring in the engineering field and eliminate the limits of traditional monitoring methods. Currently, the manufacturing of MEMS sensors is becoming increasingly mature. It has the advantages of small size, low cost, low energy consumption, easy installation, strong performance, and high monitoring data reliability. However, dam subsidence is chronic. If the MEMS sensor is directly applied to dam monitoring, we cannot guarantee the reliability of the sensor measurement data [16-17].

It is difficult to detect sluggish movement by MEMS sensors. To address this problem, this paper designs a new intelligent monitoring system based on the collaborative measurement of dual MEMS sensors, which improves the sensitivity of the monitoring system while ensuring the accuracy of the measurement data. The system uses coordinate transformation in the monitoring system to determine the endpoint coordinates of the sensor array to determine dam subsidence [18]. Then, based on a dual MEMS sensor collaborative monitoring algorithm, common compensation between sensor monitoring data is realized [19].

The rest of the paper is arranged as follows: Section 2 introduces the MEMS sensor array design scheme, Section 3 introduces the dam subsidence monitoring algorithm, Section 4 introduces the dual-sensor collaborative measurement algorithm, Section 5 describes the system composition, Section 6 describes the experimental results, and Section 7 summarizes the conclusions.

2. MEMS sensor array design scheme

The settlement monitoring system designed in this paper is mainly aimed at large earth-rock dams in plateau areas. The mechanism of settlement and deformation of earth-rock dams is relatively complicated, and there are mainly couplings: the coupling between the deformation that changes with the increase of the filling height and the aging deformation; the compression deformation generated during the filling process is caused by the dissipation of pore water pressure. The coupling effect between the resulting consolidation settlement and the soil skeleton creep under the continuous earth pressure state; the stress coupling bearing and deformation coordination effect between clay and gravel soil. The Changheba Hydropower Station in the Dadu River Basin, Sichuan, China has a total reservoir capacity of 1.075 billion

m3. The minimum elevation of the dam foundation surface is 1 457.00 m, the maximum dam height is 242.50 m, and the dam crest length is 502.85 m. The dam body is based on core wall settlement monitoring. Settlement monitoring program. In order to monitor the settlement of the core wall, the internal settlement of the core wall area is monitored by a variety of instruments. The stable performance string settler and electromagnetic settler are selected. At the same time, in order to adapt to larger settlement deformation, the innovative use of a large range potentiometer displacement meter. At the axis of the core dam, a vertical line for layered settlement observation is arranged. Settlement measuring lines of potentiometer type displacement meters are arranged on the core wall, downstream and the axis of the dam. Settlement measuring lines of potentiometer type displacement meters are arranged on the core wall and downstream. The height spacing of the measuring points is 30 m. The specific layout is shown in **Fig. 1**.

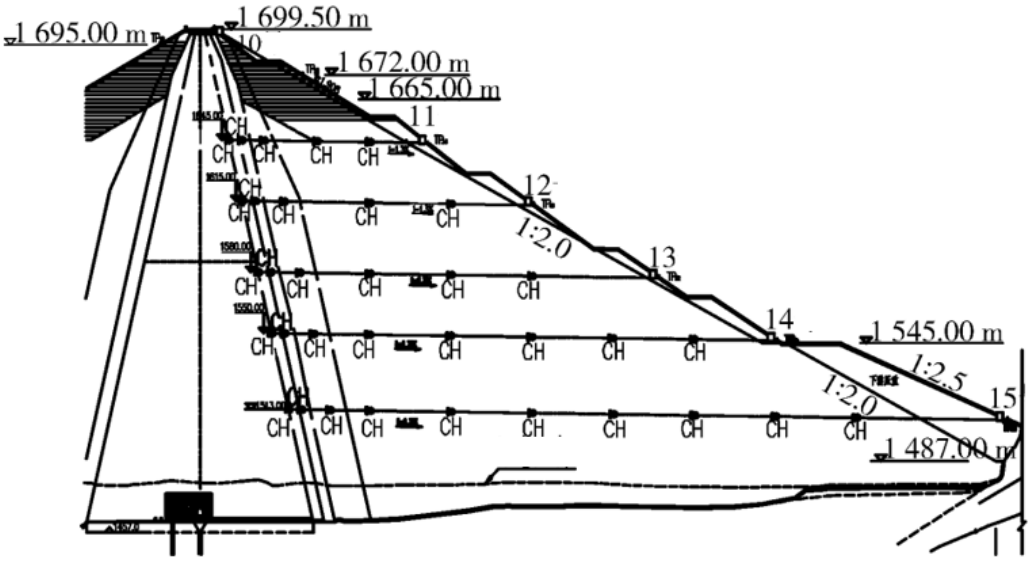

Fig. 1. Schematic diagram of dam settlement monitoring instrument layout

Multiple MEMS sensors are installed in the pipeline to form a sensor array. A linear array of equally spaced sensors and networks of other shapes can be adopted, as shown in **Fig. 2** and **Fig. 3.**

As shown in **Fig. 2** and **Fig. 3**, the blue line is the monitoring pipe, and the red line is the MEMS sensor installed in the pipe. The topological structure of the even-spaced straight-line layout scheme is relatively simple. However, when the terrain is non-flat, the sampling interval is no longer equal, resulting in no uniform sampling. In the radial sensor array scheme, recovering the original terrain from the digital signal is complicated. Moreover, as the terrain is deformed, its optimal deployment plan may no longer be ideal. Therefore, this paper adopts the equally spaced linear sensing array scheme [20].

In this type of layout, the sensor array strips are far apart. The deformation of a certain sensor array belt will not affect the adjacent sensor array, so each sensor array can be analyzed separately. The dam subsidence model is the core of the dam safety monitoring system and aims to convert the discrete data measured by the sensor array into the subsidence of the dam. To improve the measurement accuracy of the sensor array, this paper proposes a dam subsidence monitoring scheme based on two-sensor collaborative measurements.

3. Dam subsidence monitoring algorithm

3.1 The flow of the subsidence monitoring algorithm

In the measurement, the MEMS sensor cannot directly determine the displacement of dam subsidence. The displacement data are obtained by measuring the tilt angle of the carrier after movement. The accelerometer- and gyroscope-measured values are transformed into an Euler rotation matrix through information fusion. As shown in **Fig. 4**, multiple sensors form a sensor array, which is arranged inside the dam to monitor the subsidence of the dam [21].

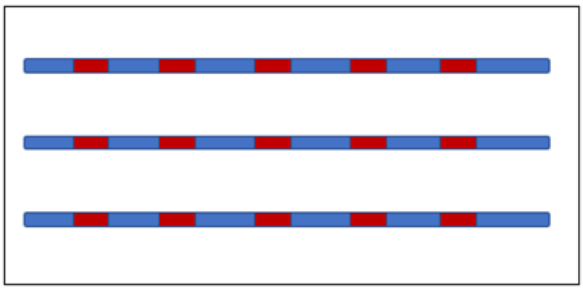

Fig. 2. Equally spaced linear sensing array scheme

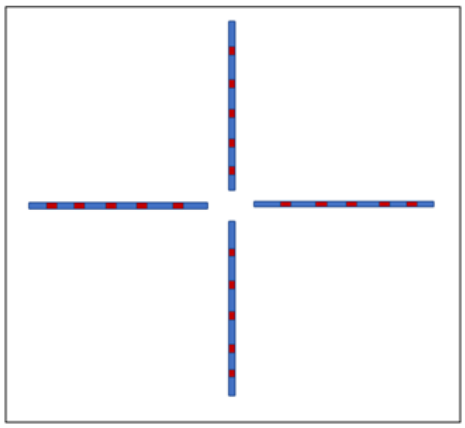

Fig. 3. Radial sensing array scheme

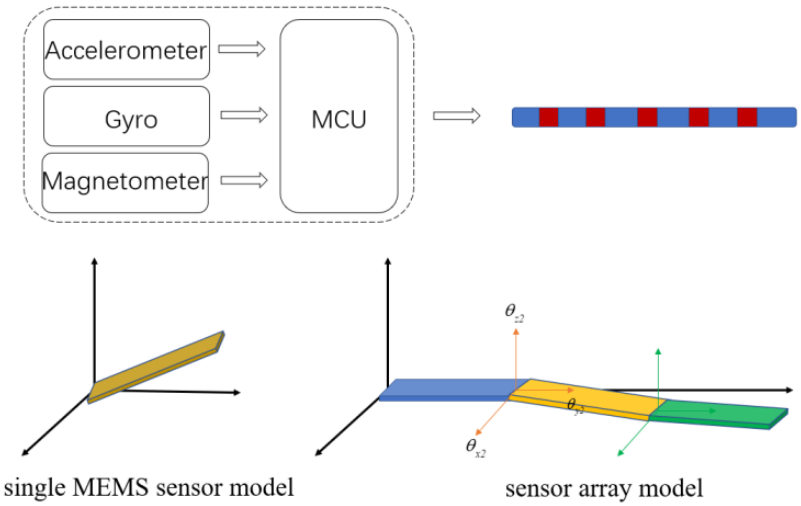

Fig. 4. Schematic of the sensor array measurement system

Assuming that the sensor array layout plane is horizontal in the dam, first, we record the initial angle of the sensor array. When the dam subsides, the sensor array will deform with the dam and then record the angle value of the rotation around each axis. Based on the above-described attitude angles, the relative rotation matrix is calculated so that we can calculate the endpointcoordinates of each segment in the array. Taking the head end of the first segment as the reference point, the subsidence is calculated as the difference between the coordinate values and the initial values. The measurement algorithm flow is shown in **Fig. 5**.

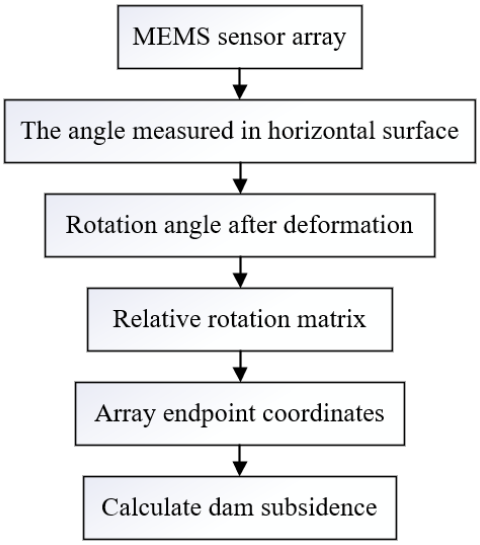

Fig. 5. Dam settlement measurement algorithm flow

3.1 Solving end point coordinates in the sensor array based on coordinate transformation

MEMS sensor arrays are equally spaced inside the dam. In the array coordinate system, the positive x-axis direction is defined as the direction in which the sensor extends, and the positive y-axis direction is defined as the direction pointing to the inside of the dam, as shown in **Fig. 6**.

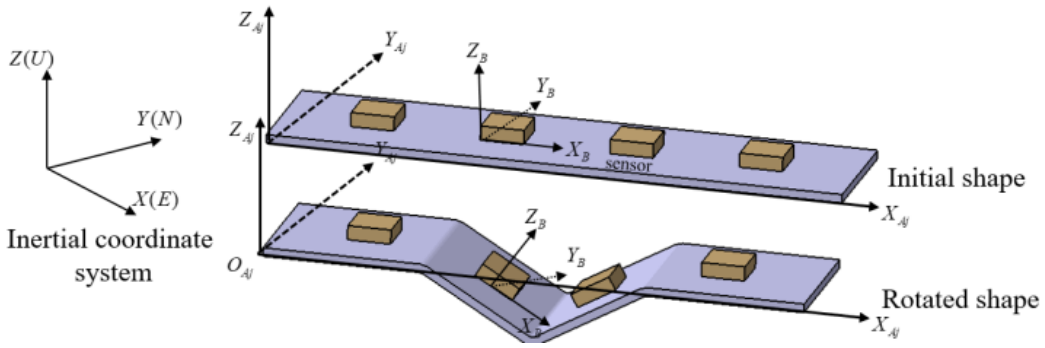

Fig. 6.1. The principle of the subsidence calculation and calculation of displacement through the tilt angles.

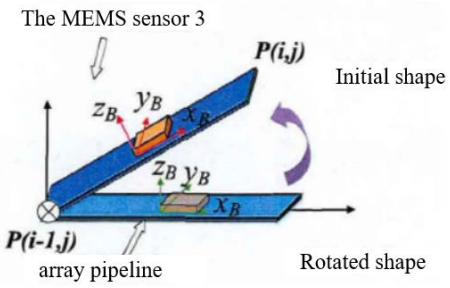

Fig. 6.2. Schematic diagram of array pipe deformation and rotationt angles.

When the sensor array is deployed on different terrains or the terrain changes, the sensor array network will be bent and twisted accordingly in space. **Fig. 6.1** is a schematic diagram of the possible bending and torsion of the first sensor array when the terrain changes. In the figure, (a) is the inertial coordinate system {G}, (b) is the initial shape of the array, and (c) is the shape of the array after the terrain is deformed. The bending and twisting of the sensor array can be transformed into the rotation of several sensors around the sensor coordinate system (or around a fixed coordinate system). The rotation sequence around the sensor coordinate system is different from that of the inertial coordinate system, and the rotation angle is the same. **Fig. 6.2** shows the bending and torsion of sensor 3. It is stipulated that the angle of rotation is positive when rotating counterclockwise around the coordinate axis; when rotating clockwise, it is negative (the same hereinafter). One segment of the sensor array (defined as $x = 0$) is fixed. The coordinate values calculated in this paper are about the fixed point of the first segment of the array. The coordinate of this fixed point is O_0 (0, 0, 0) [22].

Multiple sensor arrays are placed at equal intervals to form a sensor network. Considering the structural safety of large earth-rock dams, the sensor array designed in this paper is very slender, so the Bosch BMI055 inertial measurement device is used. Bosch BMI055 IMU is an ultra-small 6-axis inertial sensor, composed of a digital three-axis 12-bit accelerometer and a digital three-axis 16-bit gyroscope. They are installed in pairs on the flexible circuit board and placed in the array pipeline. 5 pairs of sensors are a group, and each group has a single-chip microcomputer. The interval between the sensors is determined according to the frequency of the actual terrain. In the laboratory simulation environment, the interval between the sensors is designed to be 30cm. In addition, it is required to ensure the consistency of the sensor coordinate system during deployment, that is, the coordinate axis xb of the sensor is along the direction of the sensor array. This article requires that the torsion angle of the sensor array around the xb axis is less than 60°. If the sensor array can be twisted around the xb axis (the xb axis is along the sensor array direction), it will not be able to distinguish the movement of the terrain (settlement or uplift).

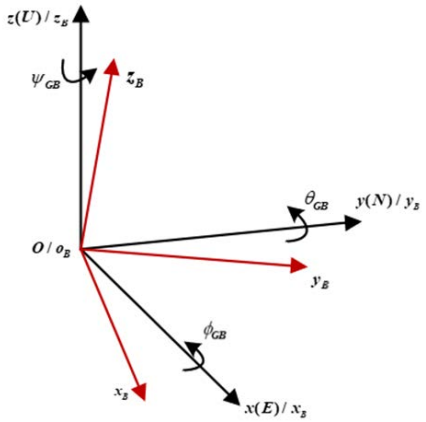

Fig. 7. Conversion relationship between the inertial coordinate system and sensor coordinate system

The angle data directly measured by the MEMS sensor are relative to the inertial coordinate system, so the coordinate system of the sensor during bending and torsion changes as follows:

1) Before measurement, the sensor coordinate system is consistent with the inertial coordinate system.

2) Rotate angle around the z_b axis.

3) Rotate angle around the rotated y_b axis.

4) Rotate angle around the x_b axis.

As shown in **Fig. 7**, the black line coordinate system directs the initial coordinate system, and the red line directs the coordinate system after rotation.

In **Fig. 7**, the rotation matrix of each step is

$$\boldsymbol{R}_z(\psi_{GB}) = \begin{bmatrix} cos(\psi_{GB}) & sin(\psi_{GB}) & 0 \\ sin(-\psi_{GB}) & cos(\psi_{GB}) & 0 \\ 0 & 0 & 1 \end{bmatrix} \tag{1}$$

$$\boldsymbol{R}_y(\theta_{GB}) = \begin{bmatrix} cos(\theta_{GB}) & 0 & sin(-\theta_{GB}) \\ 0 & 1 & 0 \\ sin(\theta_{GB}) & 0 & cos(\theta_{GB}) \end{bmatrix} \tag{2}$$

$$\boldsymbol{R}_x(\phi_{GB}) = \begin{bmatrix} 1 & 0 & 0 \\ 0 & cos(\phi_{GB}) & sin(\phi_{GB}) \\ 0 & sin(-\phi_{GB}) & cos(\phi_{GB}) \end{bmatrix} \tag{3}$$

$$\boldsymbol{R}_{AB} = \begin{bmatrix} cos\theta cos\psi' & sin\psi' cos\theta & -sin\theta \\ -sin\psi' cos\phi + cos\psi' sin\phi sin\theta & cos\theta cos\psi' + sin\psi' sin\phi sin\theta & sin\phi cos\theta \\ cos\psi' sin\theta cos\phi + sin\psi' sin\theta & -sin\theta cos\psi' + sin\theta cos\phi sin\psi' & cos\theta cos\phi \end{bmatrix} \tag{4}$$

The rotation matrix RGB of the sensor array is calculated according to (1), (2), and (3) and is $\boldsymbol{R}_{GB} = \boldsymbol{R}_x(\phi_{GB})\boldsymbol{R}_y(\theta_{GB})\boldsymbol{R}_z(\psi_{GB})$. In (4), (θ, ϕ, ψ) means $(\theta_{GB}, \phi_{GB}, \psi_{GB})$ in (1), (2), and (3). According to (4), the rotation matrix RGB is the rotation transformation relationship between the sensor coordinate system (B system) and the inertial coordinate system (G system).

By setting the mathematical model of the rotation relationship between the sensor coordinate system and the inertial coordinate system, it is also necessary to construct the array coordinate system (A system) and the sensor coordinate system (B system) rotation mathematical model. When the sensor array is arranged horizontally, ϕ_{GA} and θ_{GA} are equal to 0, and only the initial angle ψ_{GA} needs to be recorded. When the sensor array is deformed, the current angles ϕ_{GA}, θ_{GA} and ψ_{GA} are recorded [23-29]. Therefore,

$$\begin{cases} \phi_{AB} = \phi_{GB} \\ \theta_{AB} = \theta_{GB} \\ \psi_{AB} = \psi_{GB} - \psi_{GA} \end{cases} \tag{5}$$

Similarly, $\boldsymbol{R}_{GB} = \boldsymbol{R}_{AB}\boldsymbol{R}_{GA} = \boldsymbol{R}_{AB}\boldsymbol{R}_z(\psi_{GA})$ so

$$\boldsymbol{R}_{AB} = \begin{bmatrix} cos\theta cos\psi' & sin\psi' cos\theta & -sin\theta \\ -sin\psi' cos\phi + cos\psi' sin\phi sin\theta & cos\theta cos\psi' + sin\psi' sin\phi sin\theta & sin\phi cos\theta \\ cos\psi' sin\theta cos\phi + sin\psi' sin\theta & -sin\theta cos\psi' + sin\theta cos\phi sin\psi' & cos\theta cos\phi \end{bmatrix} \tag{6}$$

In (6), (θ, ϕ, ψ') means $(\theta_{GB}, \phi_{GB}, \psi_{GB} - \psi_{GA})$ in (1), (2), and (3). The point $P(i, j)$ is used to represent the endpoint coordinates of the i^{th} segment of the j^{th} sensor array. After rotation, the endpoint coordinates of each segment of the array can be calculated by the following formula:

$$\begin{cases} P(j,i) = P(j,i-1) + L \bullet R_{AB}(j,i), & i \geq 1 \\ P(j,0) = (0, j \bullet \lambda, 0), & i = 0 \end{cases} \tag{7}$$

In (7), l is the length of each array, whose coordinate is $(l,0,0)$. $P(j,0)$ is the starting point of the j-th array, and λ is the distance between the sensor arrays.

Combined with the description in this section, through the iterative calculation of equations (6) and (7), the coordinates of the array end points can be obtained to solve the subsidence of the dam, as shown in **Fig. 8**.

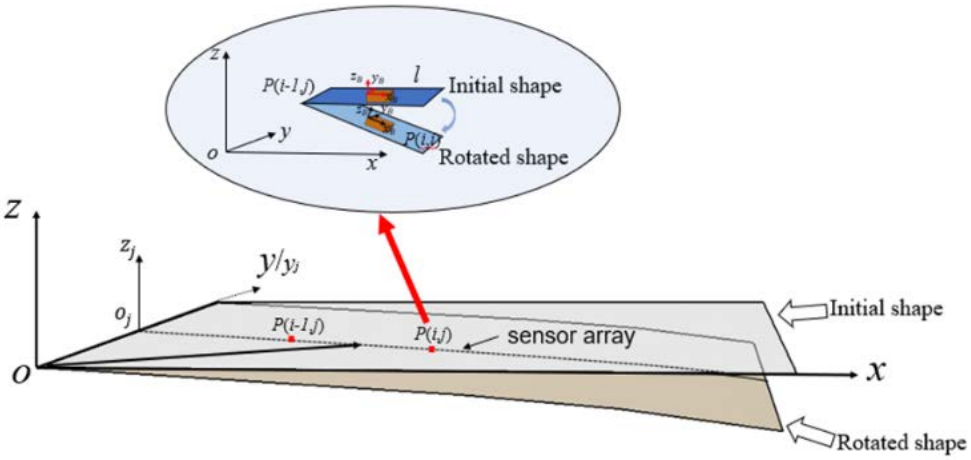

Fig. 8. Array Endpoint Solving Algorithm

4. Sensors collaborative measurement algorithm

In the traditional MEMS sensor measurement system, a single sensor is used to measure the measured carrier. In long-term monitoring, the measurement result of a single sensor accumulates a large error over time, and it is difficult to guarantee the accuracy of the measurement data. To address these problems, this paper proposes a dual-sensor cooperative measurement scheme.

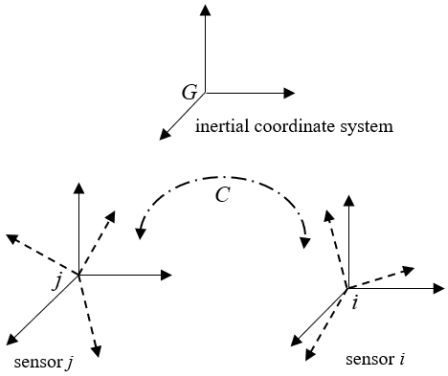

Fig. 9. Distributed sensor network system structure

In the multisensor system, multiple sensors are used to measure the same state quantity because the multisensory measurement data can compensate for each other to reduce the measurement error. Moreover, this arrangement is very conducive to sensor fault diagnosis and isolation. Two MEMS sensors on a sensor array not only displace themselves with the settling of the dam but are also affected by each other's movements. This structure is called a distributed sensor network system structure, as shown in **Fig. 9**.

In **Fig. 9**, **C** is the sensor motion transfer matrix, which can be measured when the sensor array is installed. The following can be known from the angular velocity relationship measured by the given sensors:

$$\begin{cases} \omega_{G/i} = \omega_{G/j} + \omega_{j/i} \\ \omega_{G/A} = \omega_{G/j} + \omega_{j/A} \\ \omega_{G/i} = \omega_{G/j} + \omega_{j/i} \end{cases} \tag{8}$$

Where ω is the angular velocity vector. The subscript G/i indicates the angle of the nodal system *i* relative to the inertial coordinate system G (the same follows below). Projecting (8) into the array coordinate system (A), the first equation of (8) can be changed to:

$$\boldsymbol{\Omega}_{I/i}^{j} = \boldsymbol{\Omega}_{I/j}^{j} + \boldsymbol{\Omega}_{j/i}^{j} \tag{9}$$

Where $\boldsymbol{\Omega}$ is the skew symmetric matrix of ω, and the superscript *j* represents the projection on the array coordinate system *j*. Combining the differential equation of the motion transition matrix ***C*** results in the following:

$$\boldsymbol{\Omega}_{I/i}^{j} = \boldsymbol{\Omega}_{I/A}^{j} - \boldsymbol{C}_{j}^{i}\boldsymbol{C}_{i}^{j} \tag{10}$$

Then, we obtain a mathematical model of the motion transfer matrix:

$$\begin{cases} \boldsymbol{C}_{j}^{i} = (\boldsymbol{\Omega}_{I/j}^{j} - \boldsymbol{\Omega}_{I/i}^{j})\boldsymbol{C}_{j}^{i} \\ \boldsymbol{\Omega}_{I/i}^{j} = \boldsymbol{C}_{i}^{j}\boldsymbol{\Omega}_{I/i}^{i}\boldsymbol{C}_{j}^{i} \end{cases} \tag{11}$$

In (11), $\boldsymbol{\Omega}_{I/j}^{j}$ and $\boldsymbol{\Omega}_{I/i}^{i}$ are composed of local absolute angular velocity vectors that can be obtained from the measured values of inertial nodes *i* and *j*. Equation (11) is a nonlinear matrix differential equation whose initial value can be obtained from the static matrix. $\boldsymbol{H}_i$ is defined as the installation matrix of the IMU at sensor node *i*. Then, the measured value at sensor node *i* is

$$m_i = \boldsymbol{H}_i \boldsymbol{x}_i = \boldsymbol{H}_i \boldsymbol{C}_j^i \boldsymbol{x}_j = \boldsymbol{H}_i \boldsymbol{C}_k^i \boldsymbol{x}_k \tag{12}$$

In (12), $\boldsymbol{x}_i$ is the local vector (such as acceleration and angular acceleration) in the sensor node *i* system. In the same way, m_j can be obtained. A scattered sensor network system can realize information sharing and mutual compensation for measurement data so that a dual-sensor cooperative measurement scheme can reduce measurement errors.

Each MEMS sensor group node can use inertial measurement sensors with the same or different performances or can be combined with other systems. Each node system forms a delivered network topology, and nodes can communicate with each other to realize network information sharing. In the information fusion of scattered sensor networks, each sensor node can show its own system state model without the need for a common navigation system state model. The distributed system provides a more flexible solution for designing multisensor measurement systems. It not only improves overall measurement performance but also improves sensor-level and system-level fault tolerance, provides more accurate local state estimations, and realizes automatic sensor alignment.

5. Construction of the dam subsidence monitoring system

The whole measurement system includes a sensor array, a controller, and a computer. The sensor array consists of four rigid pipes. In application, both the accuracy and the economic efficiency need to be considered. Eachrigid pipe hosts twomems sensors (BMI055) and is arranged on elastic steel tape.

The controller is a STM32 microcontroller unit (MCU) in the system. Data are acquired from the sensor array by the Inter-Integrated Circuit (IIC) bus protocol and sent to the MCU. Then, the MCU communicates with the computer software by analog-to-digital converter (ADC) module. The computer is to calculate and draw the shape curves of the array, directly showing vertical deformation and the orientation (subsidence).

6. Experimental result analysis

In the test, eight MEMS sensors are used to remodel the shapes of the array, which is composed of four segments. The sensor array is deployed inside the assimilated dam. The dam model is put in a glass box, and the MEMS sensor array is buried horizontally. To facilitate observation, the sensor array is arranged against the glass wall, and eight red marks are evenly made on the array pipe. **Fig. 10** shows the following:

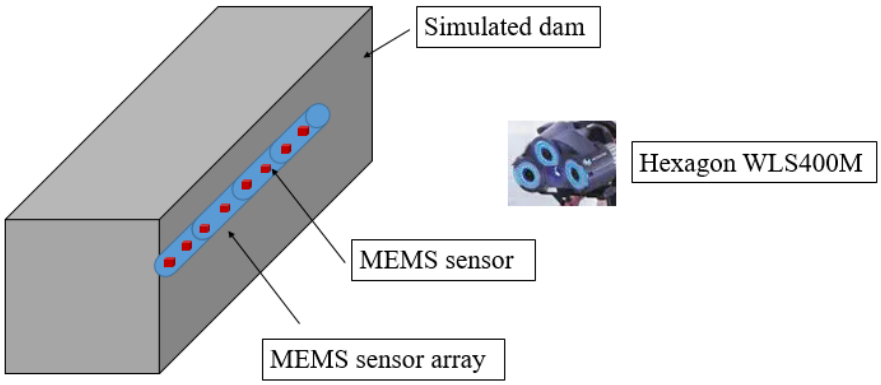

Fig. 10. Simulation experiment of dam subsidence

The Hexagon WLS400M white light measurement system adopts manual operation to realize three-dimensional measurement operation, quality inspection and digitization. The system has complete functions and can support a variety of industrial applications. The solid carbon fiber sensor structure provides stable and protective support for all optical components, ensuring high reliability under harsh environmental conditions. To support the monitoring accuracy, a Hexagon WLS400M white light scanner system is applied to observe the displacement change of the red mark on the pipeline. The accuracy of the WLS400M system is 0.03 mm. At the same time, the MEMS sensor array measures static acceleration and initial inclination, and then, the data are collected by the MCU, sent to the computer, and transferred to tilt angles. Then, the subsidence of the array are obtained according to the relationship between the tilt angles and coordinates mentioned earlier. The reference point and tested points are the same for the system designed in this paper and the Hexagon WLS400M system. The error analysis principle used for the shape reconstruction of the MEMS sensor array is shown in **Fig. 11**.

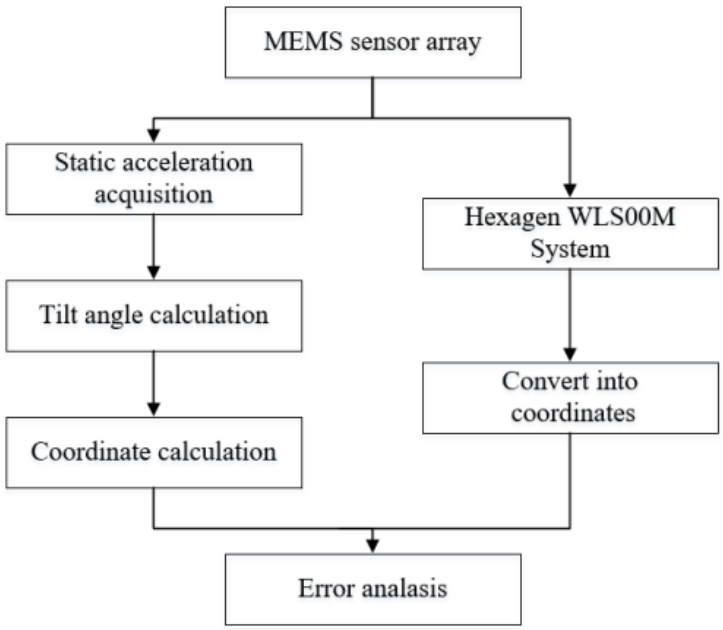

Fig. 11. Error analysis principle used by the MEMS sensor to monitor dam subsidence

Table 1. the measurement error

	Mean absolute Error (*mm*)	**Root mean square Error** (*mm*)	**Max Error** (*mm*)	**Max Subsidence** (*mm*)	**Min Subsidence** (*mm*)	**Max absolute value of tilt angle** (°)	**Min absolute value of tilt angle** (°)
1	0.95	1.5	1.04	9.11	0.53	45.22	5.22
2	0.78	0.82	0.25	7.13	0.61	25.96	4.68
3	0.16	1.17	1.55	8.91	0.84	48.03	6.26
4	0.43	1.31	1.65	8.05	1.74	43.81	4.12
5	0.68	0.91	1.07	8.90	1.06	38.97	7.11

As mentioned earlier, the initial values of the array are zero, and the displacements measured directly represent vertical subsidence. We performed five experiments that took three days each. The mean absolute error (MAE), root-mean-square error (RMSE), maximum absolute error, and maximum subsidence are adopted to analyses the measurement error, which are listed in **Table 1**. Strong agreement is proven between the measured data and the observed data. In the four shape experiments, the maximum RMSE is 1.5 mm, the maximum absolute error is 1.65 mm, and the maximum subsidence is 9.11 mm. The minimum RMSE is 2.35 mm, and the minimum absolute error is 0.16 mm, with the maximum subsidence being 6.05 mm. The maximum absolute value of the tilt angle is 48.03°, and the minimum one is 4.12°. In the computer screen, the subsidence monitoring results are presented in **Fig. 12** below.

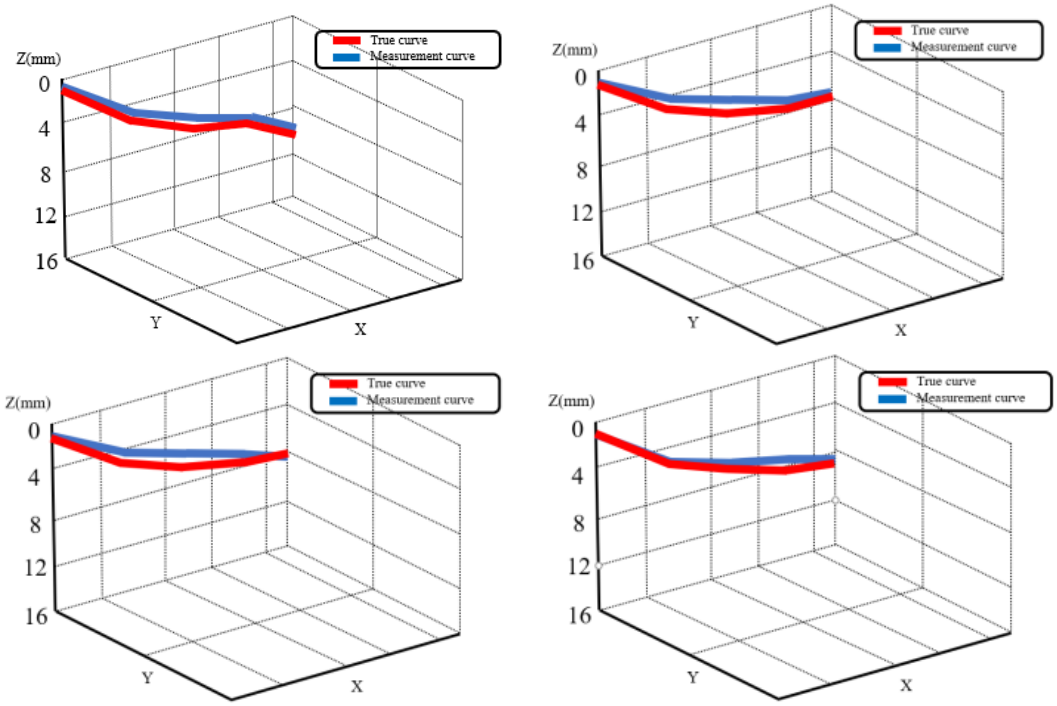

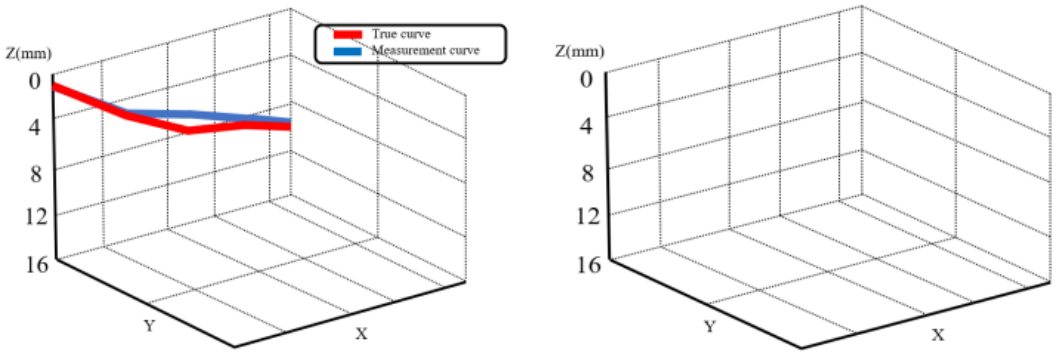

Fig. 12. The PC results

7. Conclusion

To address the requirements of the dam subsidence monitoring project, this paper analyses the disadvantages of the current engineering monitoring system and designs a dam subsidence monitoring system based on a MEMS sensor array. First, combined with a three-dimensional measurement model, a settlement measurement algorithm is proposed, which converts the resolved space bending and torsion angles into the endpoint coordinates of the sensor array and calculates terrain subsidence by the endpoint coordinates. Then, to analyses the inferiority of single-sensor measurement, this paper proposes a method of dual-sensor collaborative measurement, which improves the accuracy and reliability of the measurement data obtained by the monitoring system. Through experimental analysis, compared to conventional monitoring systems, the monitoring system proposed in this paper is more table exhibits excellent sensitivity to the slow displacement of the carrier and can effectively reduce cumulative error. In order to improve the measurement signal processing capability of the dam settlement monitoring system, our work will mainly focus on the multi-sensor information fusion algorithm. In addition, in the extreme cold environment of the plateau, in order to ensure the long-term measurement stability of the monitoring system, measuring the cold resistance and pressure resistance of the array is also the focus of the design of the monitoring array in the next stage.

Acknowledgement

This job is supported by the National key R&D Program of China under Grant NO. 2018YFB0203901 and the Key Research and Development Program of Shaanxi Province (No.2018ZDXM-GY-036) and Shaanxi Key Laboratory of Intelligent Processing for Big Energy Data (No.IPBED7).

References

[1] D Avrahami, M Patel, Y Yamaura, et al., “Unobtrusive Activity Recognition and Position Estimation for Work Surfaces Using RF-Radar Sensing,” *The ACM Transactions on Interactive Intelligent Systems*, Vol.10, No.01, pp.1-28, August 2019. Article (CrossRef Link)

[2] X Y Liao, “Research on Dam Safety Monitoring System Based on Wireless Sensor Networks,” Ph. M. Thesis, Dalian University of Technology, Dalian, China, 2012.

[3] Z R Zhao, et al., "Development status and prospect of dam safety monitoring technology at home and abroad," *Hydropower Automation and Dam Monitoring*, Vol.34, No.05, pp.52-57, June 2012.
[4] M Wieland, G F Kirchen, "Long-term dam safety monitoring of Punt dal Gall arch dam in Switzerland," *Frontiers of Structural & Civil Engineering*, Vol.6, No.01, pp.76-83, March 2012. Article (CrossRef Link)
[5] C H Loh, C H Chen, T Y. Hsu, "Application of advanced statistical methods for extracting long-term trends in static monitoring data from an arch dam," *Structural Health Monitoring*, Vol.10, No.06, pp.587-601, November 2011. Article (CrossRef Link)
[6] C Serra, A L Batista, A. Tavares, "Creep of dam concrete evaluated from laboratory and in situ tests," *Strain*, Vol.48, No.03, pp. 241-255, June 2012. Article (CrossRef Link)
[7] C H See, K V Horoshenkov, et al., "A low power wireless sensor network for gully pot monitoring in urban catchments," *Sensors Journal*, Vol.12, No.05, pp. 1545-1553, May 2012. Article (CrossRef Link)
[8] S Kim, D Tasse, A K Dey, "Making Machine-Learning Applications for Time-Series Sensor Data Graphical and Interactive," *The ACM Transactions on Interactive Intelligent Systems*, Vol.07, No.02, pp.1-30, July 2017. Article (CrossRef Link)
[9] D Kim, D Kim, S An, "Communication Pattern Based Key Establishment Scheme in Heterogeneous Wireless Sensor Networks," *Ksii Transactions on Internet & Information Systems*, Vol.10, No.03, pp.1249-1272, March 2016. Article (CrossRef Link)
[10] H. Ceylan, et al., "A Feasibility Study on Embedded Micro-Electromechanical Sensors and Systems (MEMS) for Monitoring Highway Structures," *Construction and Building Materials*, Vol.23, No.02, pp.111-120, June 2011. Article (CrossRef Link)
[11] C Li, "Study of Accelerometer data fusion in monitoring of ground subsidence induced by tunnel construction," *Journal of Engineering Geology*, Vol.25, No.01, pp.60-67, July 2017. Article (CrossRef Link)
[12] Y B. Lin, J S. Lai, K C. Chang, et al., "Using MEMS sensors in the bridge scour monitoring system," *Journal of the Chinese Institute of Engineers*, Vol.33, No.01, pp. 25-35, May 2010. Article (CrossRef Link)
[13] H C Zhu, "Research on submarine terrain deformation monitoring system based on MEMS sensing arrays and its data acquisition synchronization technology," Ph. M. Thesis, Zhejiang University, Hangzhou, China, 2019.
[14] F C Liu, X Zhi, Z H Liu, "Application of SAA on slope deformation monitoring of pumped storage power station," *Dam and Safety*, Vol.00, No.01, pp.22-25, 36, January 2020. Article (CrossRef Link)
[15] C Liao, "Study of Applying Fiber Optic Gyro Strapdown Inertial Navigation," Ph. M. Thesis, China Three Gorges University, Yichang, China, 2016.
[16] A Sabato, "Presentation-Pedestrian bridge vibration monitoring using a wireless MEMS accelerometer board," in *Proc. of 2015 IEEE 19th International Conference on Computer Supported Cooperative Work in Design (CSCWD)*, Calabria, Italy, pp.437-442, September 2015. Article (CrossRef Link)
[17] M Pandit, A Mustafazade, C Zhao, et al., "An Ultra-High-Resolution Resonant MEMS Accelerometer," in *Proc. of 2019 IEEE 32nd International Conference on Micro Electro Mechanical Systems (MEMS)*, Seoul, Korea (South), pp. 664-667, September 2019. Article (CrossRef Link)
[18] Y Liu, G Xiang, Y Lu, et al., "Calibration of MEMS Accelerometer Based on Kalman Filter and the Improved Six Position Method," *Journal of Communications*, Vol. 11, No.05, pp.516-522, May 2016. Article (CrossRef Link)
[19] C Y Xu, J W Chen, H C Zhu, et al., "Experimental Study on Seafloor Vertical Deformation Monitoring Based on MEMS Accelerometer Array," in *Proc. of The 28th International Ocean and Polar Engineering Conference*, Sapporo, Japan, June 2018. Article (CrossRef Link)
[20] C Y Xu, J W Chen, Y Q Ge, et al., "Monitoring the vertical changes of a tidal flat using a MEMS accelerometer array," *Applied Ocean Research*, Vol. 101, pp.102-186, August 2020. Article (CrossRef Link)

[21] C Y Xu, J W Chen, H C Zhu, et al., "Experimental Research on Seafloor Mapping and Vertical Deformation Monitoring for Gas Hydrate Zone Using Nine-Axis MEMS Sensor Tapes," *IEEE Journal of Oceanic Engineering*, Vol.44, No.04, pp.1090-1101, Oct. 2019. Article (CrossRef Link)
[22] W J Wu, Z Li, J Q, Liu, et al., "A nano-g MEMS accelerometer for earthquake monitoring," in *Proc. of 2017 19th International Conference on Solid-State Sensors, Actuators and Microsystems (TRANSDUCERS)*, Kaohsiung, Taiwan, pp. 599-602, June 2017. Article (CrossRef Link)
[23] Bin Zhou, Dawid Polap, and Marcin Wozniak, "A regional adaptive variational PDE model for computed tomography image reconstruction," *Pattern Recognition*, Vol.92, pp.64-81, March 2019. Article (CrossRef Link)
[24] Xia X, Marcin W, Fan X, Damasevicius R., Li Y, "Multi-sink distributed power control algorithm for Cyber-physical-systems in coal mine tunnels," *Computer Networks*, Vol.161, pp.210-219, Apirl 2019. Article (CrossRef Link)
[25] H Song, W Li, P Shen, A Vasilakos, "Gradient-driven parking navigation using a continuous information potential field based on wireless sensor network," *Information Sciences*, Vol.408, no.2, pp.100-114, April 2017. Article (CrossRef Link)
[26] Xu Q, Wang L, Hei XH, Shen P, Shi W, Shan L, "GI/Geom/1 queue based on communication model for mesh networks," *International Journal of Communication Systems*, Vol. 27, No. 11, pp. 3013-3029, Nov. 2014. Article (CrossRef Link)
[27] X Fan, H Song, J Yang, "Imperfect information dynamic stackelberg game-based resource allocation using hidden Markov for cloud computing," *IEEE Transactions on Services Computing*, Vol.11, no.1, pp.78-89, Jan.-Feb. 1 2018. Article (CrossRef Link)
[28] J Su, H Song, H Wang, X Fan, X, "Cdma-based anti-collision algorithm for epc global c1 gen2 systems," *Telecommunication Systems*, Vol.67, pp. 63-71, May 2018. Article (CrossRef Link)
[29] H G Min, E T Jeung, "Complementary filter design for angle estimation using mems accelerometer and gyroscope, Department of Control and Instrumentation," *Changwon National University*, Changwon, Korea, pp. 641-773, June 2015.

Tao Tao, currently is a Ph.D. in Information and Communication Engineering from Wuhan University. His research interests include computer vision, deep learning, Intelligent signal processing and brain-computer interface.

Jianfeng Yang, currently is an associate professor of Wuhan University. He received his Bachelor degree, Master degree and Ph.D. in Information and Communication Engineering from Wuhan University in July 1998, 2002 and July 2009. He worked as visiting scholar in Intel Company in 2012 and senior research associate in Northwestern University from 2015 to 2016. His research interests are in Embedded System Design, Big Data and high reliability real time wireless communication.

Dr. Wei Wei is an associate professor of School of Computer Science and Engineering, Xi'an University of Technology, Xi'an 710048, China. He is a senior member of IEEE, CCF. He received his Ph.D. and M.S. degrees from Xian Jiaotong University in 2011 and 2005, respectively. He ran many funded research projects as principal investigator and technical members. His research interest is in the area of wireless networks, wireless sensor networks Application, Image Processing, Mobile Computing, Distributed Computing, and Pervasive Computing, Internet of Things, Sensor Data Clouds, etc. He has published around one hundred research papers in international conferences and journals. He is an editorial board member of FGCS, IEEE Access, AHSWN, IEICE, KSII, etc. He is a TPC member of many conferences and regular reviewer of IEEE TPDS, TVT, TIP, TMC, TWC, JNCA and many other Elsevier journals.

MARCIN WO´ ZNIAK received diplomas in applied mathematics and computational intelligence, Master Degree in 2007 from the Silesian University of Technology and PhD in 2012 from the Czestochowa University of Technology. He is an Assoc. Professor at Institute of Mathematics of the Silesian University of Technology in Gliwice, Poland. In his scientific career, he was visiting University of WÅ´ srzburg, Germany in 2007 (for part of the studies), University of Lund, Sweden in 2016 (as a guest from the ministerial program for young research professors) and University of Catania, Italy in 2015 and 2017 (as invited professor for research projects and grants). His main scientific interests are neural networks with their applications together with various aspects of applied computational intelligence. He is a scientific supervisor in editions of "the Diamond Grant" and "The Best of the Best" programs for highly gifted students from the Polish Ministry of Science and Higher Education. Marcin Wo´zniak was/is organizer and session chair on various international conferences and symposiums, like IEEE SSCI, IEEE FedCSIS, APCASE, ICIST, ICAISC, WorldCIST.

Rafał Scherer received his MSc degree in computer science from the Czestochowa University of Technology, Poland, in 1997 and his PhD in 2002 from the same university. Currently, he is an associate professor at Czestochowa University of Technology. His present research interests include machine learning and neural networks for image processing, computer system security, prediction and classification.

ROBERTAS DAMAŠEVI ˇ CIUS graduated at the Faculty of Informatics, Kaunas University of Technology (KTU) in Kaunas, Lithuania in 1999, where he received a B.Sc. degree in Informatics.He finished his M.Sc. studies in 2001 (cum laude), and he defended his Ph.D. thesis at the same University in 2005. Currently, he is a Professor at Software Engineering Department, KTU and lectures robot programming and software maintenance courses. His research interests include brain-computer interface, bioinformatics, data mining and machine learning. He is the author or co-author of over 100 papers as well as a monograph published by Springer.